Incorporating GTV Information in a Multi-stage Process to Improve Automatically Generated Field Apertures for Rectal Cancer Radiotherapy

K. Huang[1,2], P. Das[3], L. Zhang[2], M. Amirmazaheri[2], C. Nguyen[2], D. Rhee[1,2], T. Netherton[1,2], S. Beddar[2], T. Briere[2], D. Fuentes[4], E. Holliday[3], L. Court[2], C. Cardenas[2]

[1]The University of Texas MD Anderson Cancer Center UTHealth Graduate School of Biomedical Sciences, Houston, Texas, 77030, USA

Department of [2]Radiation Physics, [3]Radiation Oncology and [4]Imaging Physics, The University of Texas MD Anderson Cancer Center, Houston, Texas, 77030, USA

JULY 12–16 2020 VIRTUAL JOINT AAPM | COMP MEETING
EASTERN TIME [GMT-4]

INTRODUCTION

Colorectal cancers are the third leading cause of cancer death for both male and female patients with over 40,000 new cases of rectum cancer each year in the United States.[1] The standard of care incorporates neoadjuvant radiotherapy treatment for improved management. Three-dimensional conformal radiotherapy (3D-CRT) is an established technique for rectal cancer with clear and algorithmic steps to produce clinical plans.[2] The planning for 3D-CRT technique depends largely on gross tumor volume (GTV) and anatomical landmarks. This study demonstrated the feasibility of automatic, 3D-CRT treatment planning for rectal cancer.

AIM

To automatically generate clinically acceptable field apertures and radiotherapy plans for rectal cancer, based on clinical GTV contours.

METHOD

- Standard rectal cancer radiation treatments use a three-field first course (PA, opposed laterals) and a two-field cone down (opposed laterals).
- Clinically, these field apertures are primarily determined by bony landmarks and GTV extent (3) as seen in digitally reconstructed radiographs (DRRs).

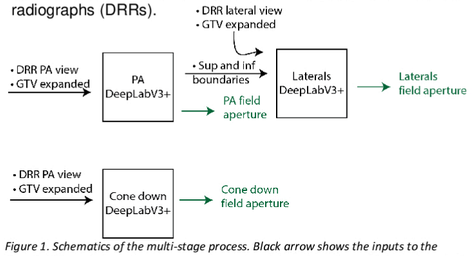

Figure 1. Schematics of the multi-stage process. Black arrow shows the inputs to the DeepLabV3+ models, and green arrow shows the outputs. Superior and inferior boundaries of the PA prediction were inputted to the Lateral model.

- To mirror this field generation process automatically, a multi-stage DeepLabV3+ network(3) was trained, validated and tested on 501 patients (301/100/100, respectively). (See Figure 1)
- First, a model was trained for the PA field using DRRs and projected GTVs as inputs.
- Second, a model was trained for the lateral fields using the output from the PA model together with DRRs and projected GTVs. This multi-stage approach incorporates additional information provided by the PA view to the lateral model.
- Third, another model was trained for the cone down fields using DRRs and projected GTVs as inputs.
- A script was written to automatically setup beams, and multi-leaf collimator, and perform final dose calculation.

RESULTS

- The multi-stage process predicted field apertures and generated plans successfully for all test patients.
- Figure 2 shows an example of the predicted target field compared with the clinical field placement.
- To mimic the clinical practice, the clinically drawn GTVs were expanded uniformly either by 2 or 3 cm (for PA).
- The predicted fields successfully placed the inferior aperture at 3 cm inferior of GTV or the bottom of obturator foramen whichever is lower (Figure 2A).

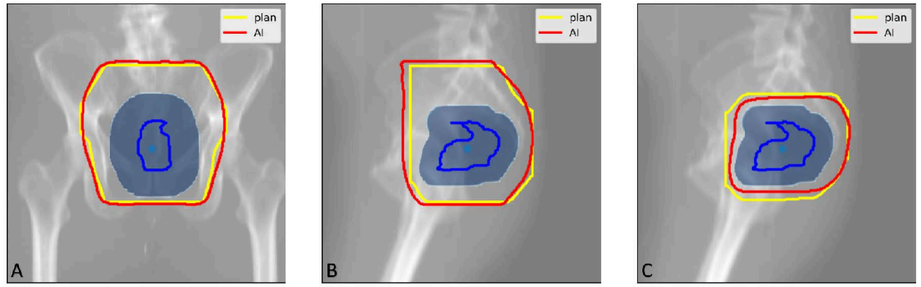

Figure 2. An example of the predicted target fields (in red) compared with the clinical target fields (in yellow) for (A) PA fields, (B) left lateral field, and (C) left lateral cone down field. DRRs (the background) and uniformly expanded GTV (the shaded blue area) are the inputs to models for PA and boost fields. The superior and inferior field edges of the PA fields were also used as inputs for the lateral field model. The GTV was uniformly expanded by 3 cm (for PA) or 2 cm (for laterals and boost). The right lateral fields are not shown as they are mirror images of the corresponding left lateral fields.

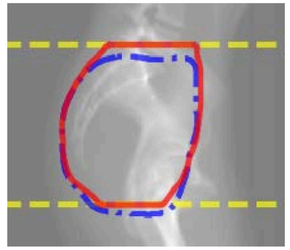

Figure 3. An example of predicted lateral target fields from models either using (in red) or not using (in dotted blue) the additional information from the PA model. The additional information from PA model was the locations of the predicted superior and inferior borders marked by the dotted yellow horizontal lines. This shows the benefit of using a multi-stage process. Leveraging the output from the PA model, the lateral model predicted fields that showed improved consistency and less ambiguity regarding the locations of the superior and inferior edges.

- The lateral model predicted more consistent field edges (superior and inferior) as the corresponding PA field, when using the multi-stage process compared to the predictions that did not use the additional inputs from PA fields (Figure 3).

- Target field prediction achieved average Dice coefficient of 0.96±0.02, 0.93±0.02, and 0.90±0.06 for PA, lateral fields and cone down fields, respectively.
- The average Hausdorff distances were 1.01±0.46, 1.67±0.78, and 1.72±0.93 cm for PA, lateral fields and cone down fields, respectively.
- The lateral model predicted more consistent field edges (superior and inferior) as the corresponding PA field, when using the multi-stage process compared to the predictions that did not use the additional inputs from PA fields (Figure 3).
- This was because in clinical practices, the superior and inferior borders of PA and laterals are kept the same. Using the output of the PA prediction for superior and inferior borders mimics this clinical practice.
- This plan used initial beam weighting of 2:1:1 for PA versus two lateral fields, and 1:1 for cone downs. The laterals and cone downs used 45° and 15° wedges, respectively. User only had to manually place wedges, and modify beam weights, as those actions are not directly scriptable in RayStation 9A.
- The entire planning process (including beam generation and dose calculation) took less than 13 min on average.

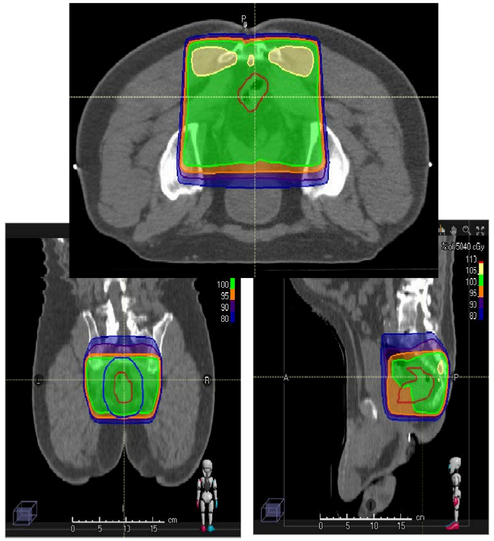

Figure 4 shows calculated dose distribution based on the predicted target fields in Figure 4. A script was used to automatically import predicted target fields, set up beams, configure dose grid, and calculate dose into the treatment planning system, RayStation 9A.

CONCLUSIONS

We developed a multi-stage process mimicking the clinical workflow for rectal radiotherapy treatment planning. This automated process can successfully generate field apertures with high fidelity and can improve treatment planning efficiency.

We used uniformly expanded GTV volume as a part of the inputs, as the placement of the field edges are determined not only by bony landmarks, but also the location and extent of the GTV volumes.

The multi-stage process offers a quick way to reduce the amount of post-processing required to align the superior and inferior borders of the PA and opposed-lateral fields.

The entire process can be completed within 13 minutes including field generation, plan optimization, and dose calculation.

For future studies, we aim to replace clinically drawn contours with automatic GTVs. Additional, we will incorporate clinical target volume to verify all the clinical tumor volumes are included in the field apertures. We also plan to develop a general field-in-field solution that is independent of treatment planning system (TPS). This will offer opportunities to accommodate patients with rectal cancer whose plans can be better prepared with field-in-field technique rather than using dynamic wedges. In addition, the planning time will be greatly reduced as the entire treatment planning process can be automated regardless of TPS' support for scripting.

ACKNOWLEDGEMENTS

Research performed under a IRB approved protocol # PA6-0379. Authors would like to thank Nicolette Taku, Adenike M Olanrewaju, and Evangeline Hillebrandt for their generous support and advice.

REFERENCES

1. Siegel RL, Miller KD, Jemal A. Cancer statistics, 2019. CA Cancer J Clin. 2019;69(1):7-34.

2. Patel SA, Wo JY, Hong TS. Advancing Techniques of Radiation Therapy for Rectal Cancer. Seminars in Radiation Oncology. 2016;26(3):220-5.

3. Minsky BD. Pelvic Radiation Therapy in Rectal Cancer: Technical Considerations. Semin Radiat Oncol. 1993;3(1):42-7.

4. Chen L-C, Zhu Y, Papandreou G, Schroff F, Adam H. Encoder-Decoder with Atrous Separable Convolution for Semantic Image Segmentation. arXiv e-prints [Internet]. 2018 February 01, 2018:[arXiv:1802.02611 p.]. Available from: https://ui.adsabs.harvard.edu/abs/2018arXiv180202611C.

CONTACT INFORMATION

For further information please contact khuang5@mdanderson.org

Click on the QR code to visit our group website.